

Direct Polymerization of the Arsenic Drug PENAO to obtain Nanoparticles with high Thiol-Reactivity and Anti-Cancer Efficiency

Janina-Miriam Noy, Hongxu Lu, Philip Hogg, Jia-Lin Yang, and Martina H. Stenzel

Bioconjugate Chem., **Just Accepted Manuscript** • DOI: 10.1021/acs.bioconjchem.8b00032 • Publication Date (Web): 18 Jan 2018

Downloaded from <http://pubs.acs.org> on January 18, 2018

Just Accepted

“Just Accepted” manuscripts have been peer-reviewed and accepted for publication. They are posted online prior to technical editing, formatting for publication and author proofing. The American Chemical Society provides “Just Accepted” as a free service to the research community to expedite the dissemination of scientific material as soon as possible after acceptance. “Just Accepted” manuscripts appear in full in PDF format accompanied by an HTML abstract. “Just Accepted” manuscripts have been fully peer reviewed, but should not be considered the official version of record. They are accessible to all readers and citable by the Digital Object Identifier (DOI®). “Just Accepted” is an optional service offered to authors. Therefore, the “Just Accepted” Web site may not include all articles that will be published in the journal. After a manuscript is technically edited and formatted, it will be removed from the “Just Accepted” Web site and published as an ASAP article. Note that technical editing may introduce minor changes to the manuscript text and/or graphics which could affect content, and all legal disclaimers and ethical guidelines that apply to the journal pertain. ACS cannot be held responsible for errors or consequences arising from the use of information contained in these “Just Accepted” manuscripts.

Direct Polymerization of the Arsenic Drug PENAO to obtain Nanoparticles with high Thiol-Reactivity and Anti-Cancer Efficiency

Janina-Miriam Noy^a, Hongxu Lu^a, Philip J. Hogg^b, Jia-Lin Yang^c, and Martina Stenzel^{*a}

^a School of Chemistry, Centre for Advanced Macromolecular Design (CAMD), University of New South Wales, Kensington, Sydney, NSW 2052, Australia

^b The Centenary Institute and National Health and Medical Research Council Clinical Trials Centre, University of Sydney, Sydney, Australia

^c Lowy Cancer Research Centre and Prince of Wales Clinical School, University of New South Wales, Kensington, Sydney, NSW 2052, Australia

*E-mail: m.stenzel@unsw.edu.au

Abstract

PENAO (4-(N-(S-penicillaminylacetyl)amino) phenylarsonous acid), which is a mitochondria inhibitor that reacts with adenine nucleotide translocator (ANT), is currently being trialed in patients with solid tumors. To increase the stability of the drug, the formation of nanoparticles has been proposed. Herein, the direct synthesis of polymeric micelles based on the anti-cancer drug PENAO is presented. PENAO is readily available for amidation reaction to form PENAO MA (4-(N-(S-penicillaminylacetyl) amino) phenylarsonous acid methacrylamide) which undergoes RAFT (reversible addition fragmentation chain transfer) polymerization with poly(polyethylene glycol methyl ether methacrylate) (PEGMA) as comonomer and poly(methylmethacrylate) (pMMA) as chain transfer agent, resulting in p(MMA)-*b*-p(PEG-*co*-PENAO) block copolymers with 3-15 wt.% of PENAO MA. The different block copolymers self-assembled into micelle structures, varying in size and stability ($D_h = 84 - 234$ nm, $cmc = 0.5 - 82 \mu\text{g mol}^{-1}$) depending on the hydrophilic to hydrophobic ratio of the polymer blocks and the amount of drug in the corona of the particle. The more stable micelle structures were investigated towards 143B human sarcoma cells, showing an enhanced cytotoxicity and cellular uptake compared to the free drug PENAO (IC_{50} (PENAO) = $2.7 \pm 0.3 \mu\text{M}$; IC_{50} (micelle M4) = $0.8 \pm 0.02 \mu\text{M}$). Furthermore, PENAOs arsenous acid residue remains active when incorporated into a polymer matrix and conjugates to small mono and closely spaced dithiols and is able to actively target the mitochondria, which is PENAO's main target to introduce growth inhibition in cancer cells. As a result, no cleavable linker between drug and polymer was necessary for the delivery of PENAO to osteosarcoma cells. These findings provide a rationale for *in vivo* studies of micelle M4 versus PENAO in an osteosarcoma animal model.

Introduction

Metal-based drugs have been used as therapeutic agents since the early days of civilisation¹. Paul Ehrlich kick-started their success in 1910 with the development of the first chemotherapeutic Salvarsan, an arsenical that was used for the treatment of syphilis and African trypanosomiasis (sleeping sickness).² But it was not only his work that influenced the modern metal-based medicine in the 20th century; many other scientists including Robert Koch³, Francis Dwyer⁴⁻⁵, and particularly Barnet Rosenberg⁶ are noteworthy for their discovery of the bacteriostatic and anticancer properties of gold salts, ruthenium polypyridyl complexes, and platinum amine complexes.

In addition to the above mentioned metal compounds, arsenic-based composites have proven to be remarkable candidates for biomedical applications due to their binding ability with thiolates of cysteine residues. Particularly the stable cyclic dithioarsinite complexes formed between arsenic (III) and closely spaced protein thiols, which results in deactivation of the protein's function.⁷⁻⁹ Arsenic-thiol conjugation reaction has been well studied over the last years^{7, 10-14}, and has been used to its advantages: Peng *et al.* recently demonstrated that arsenic trioxide can be loaded onto folate labeled human-serum-albumin by arsenic-sulfur bond formation, which facilitates the therapeutic effect of arsenic trioxide on chronic myeloid leukemia and xenograft tumor models.¹⁵ Inorganic arsenic trioxide is still the most effective drug against acute promyelocytic leukemia (APL) up to date.⁷

A promising cancer therapeutic is the hydrophilic organoarsenical PNAO (4-(N-(S-penicillaminylacetyl)amino) phenylarsonous acid) which is emphasized in this work, and was developed by Hogg and co-workers.¹⁶ It is currently being trialed in a phase I/IIa dose escalation study in patients with solid tumors. PNAO is a second generation trivalent arsenical mitochondria inhibitor from GSAO (4-(N-(S-glutathionylacetyl)amino) phenylarsonous acid) that deactivates the mitochondrial adenine nucleotide translocator (ANT) by forming a stable cyclic dithioarsinite complex with ANT cysteines 57 and 257.¹⁷ PNAO has demonstrated to have an anti-tumor growth effect on many tumors with negligible side-effects at efficacious doses.^{16, 18-19}

However, the efficacy of arsenical-based drugs and most other metal-based drugs is limited by several factors such as low drug solubility, high systemic toxicity, development of drug resistance, and rapid deactivation by complexation with proteins or oxidation reactions. For instance, despite PNAO's clinical success, its accumulation rate depends on rate of export by the MDR (multidrug resistance) protein MRP1/2 and efficacy on the cellular levels of glutathione. By inhibiting MRP1/2 and blocking de novo synthesis of glutathione, PNAO's cell growth inhibition decreased drastically (from $IC_{50} = 1100$ nM to $IC_{50} = 20$ nM) in bovine aortic endothelial (BAE) cells.¹⁶

1
2
3 To overcome many of these limitations, nanocarriers have been developed. The delivery of
4 therapeutic compounds using nanotechnology has been widely proposed to improve the solubility
5 and efficacy, while alleviating the side effects of chemotherapeutic agents by altering their
6 pharmacokinetics and biodistribution. The delivery of chemotherapeutics *via* nanocarriers has
7 shown to prolong circulation time in the blood stream, to increase the specific retention in solid
8 tumour tissue (enhanced permeability and retention (ERP) effect)²⁰⁻²¹, and to avoid the recognition
9 by the mononuclear phagocyte system.²²⁻²³

10
11
12
13
14 Much attention has been drawn to nanoparticle systems for the delivery of inorganic arsenite or
15 arsenous acid, which are highly toxic to normal tissue. Many of these nanoparticle formulations
16 improved drug selectivity to diseased tissue, tumor suppression efficacy by alleviating systemic
17 toxicity,²⁴⁻²⁵ drug loading efficiency²⁶, and drug accumulation rate in cancer tissues²⁷⁻³⁰.

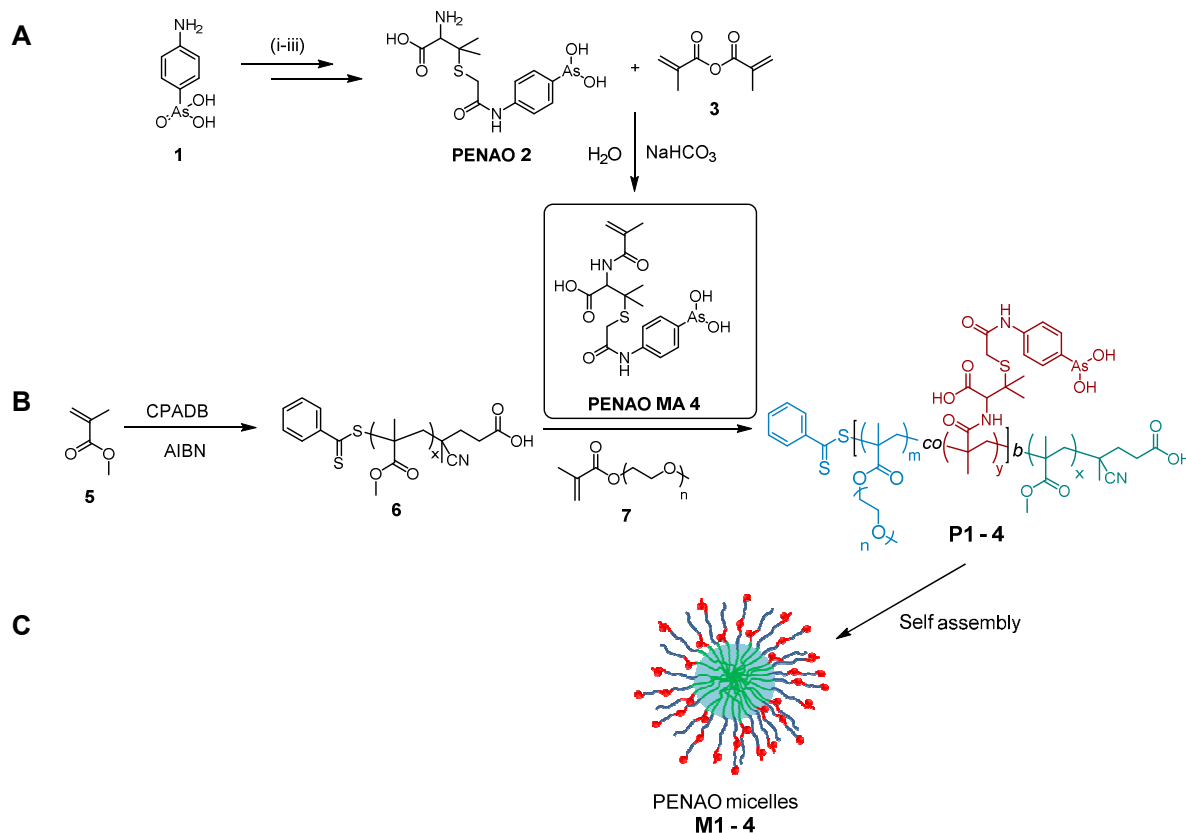
18
19
20 Most notable for these abovementioned nanocarriers is that they were all prepared by physical
21 encapsulation of the arsenical compound. Physical entrapment is easy to implement and versatile
22 for many agents, specifically hydrophobic drugs. However, the loading efficiency is generally low and
23 drugs can easily leak out of the nanoparticle into the blood stream. In this work, we therefore
24 applied chemical conjugation of the arsenic drug PENA0 to a polymeric micelle to avoid drug leakage
25 and premature release.

26
27
28
29
30
31
32
33
34
35
36
37
38
39
40
41
42
43
44
45
46
47
48
49
50
51
52
53
54
55
56
57
58
59
60
Polymeric micelle systems can be formed from amphiphilic polymers that self-assemble above the
critical micelle concentration (cmc) to core – shell structures. The core is built up by the hydrophobic
part of the block copolymer, allowing to solvate hydrophobic components, while the shell (or
corona) is equivalent to the hydrophilic segment of the block copolymer, and therefore responsible
for its high water-solubility.³¹

Most anti-cancer drugs are of hydrophobic nature and therefore favor the hydrophobic environment
of the core. When chemical drug-polymer conjugation is utilized, a cleavable linker is often
necessary to enable drug release inside the tumors.³² By using hydrophilic drugs which assemble on
the corona of a micelle, a cleavable linker may not be mandatory. Moreover, specific drug molecules
can act as ligands to increase the probability to interact with its target. Nevertheless, the
conjugation of drugs or ligands on nanoparticle surfaces can implicate difficulties: Stability, size and
immunogenicity are often affected by the attachment of molecules. In addition, conjugated
hydrophilic drugs may exhibit unfavourable pharmacokinetics in terms of absorption, distribution,
and metabolism.³³ However, due to the insufficient availability of hydrophilic drugs, little is known
about their effect on micelle surfaces.

Herein we describe the direct synthesis of polymers, based on the organoarsenical drug PENA0,
which were then self-assembled into polymeric micelle structures, as shown in **Scheme 1**. As PENA0

acts by reacting with thiols, the activity of the prepared polymers and micelles were tested using different small synthetic mono and closely spaced dithiols. The micellar delivery systems were tested *in vitro* on 2D monolayer cell culture to determine whether PENAO based polymeric nanoparticle's cytotoxicity and cellular uptake will have an appreciable outcome towards human 143B osteosarcoma cells. As the mitochondria is the intended target for the PENAO based polymeric nanoparticles, their cellular localization was analyzed using confocal microscopy. Although the focus of this work is to deliver the drug PENAO, it also provides a better understanding of the effect of hydrophilic drugs on micelle surfaces. Furthermore, the micelle systems can be used in future as reactive scaffold for cyclic peptides.



Scheme 1. (A) Synthesis of PENAO MA 4: (i-iii) Synthesis of PENAO: (i) *p*-arsanilic acid **1** was reacted with bromoacetyl bromide to obtain the precursor BRAA. (ii) BRAA was reduced with HBr, NaI and H₂SO₄ to BRAO. (iii) PENAO **2** was synthesized from BRAO and *D*-penicillamine. PENAO was then reacted with methacrylic anhydride **3** to PENAO MA **4**. (B) Synthesis of p(MMA)-*b*-p(PEG-*co*-PENAO) block copolymers **P1 – 4** via the RAFT process using p(MMA) macro RAFT agents **6**. (B) Formation of PENAO micelles (**M1 – 4**) via self-assembly.

Results and Discussion

PENAO monomer synthesis

The drug PENAO (4-(*N*-(*S*-penicillaminylacetyl) amino) phenylarsonous acid) **2** was obtained following the three-step procedure of Dilda *et al.*¹⁶ with minor modifications, resulting in 74 % yield of drug. The PENAO monomer (4-(*N*-(*S*-penicillaminylacetyl) amino) phenylarsonous acid methacrylamide, PENAO MA, **4**) was synthesized *via* a nucleophilic substitution reaction of the secondary amine from PENAOs amino acid residue and methacrylic anhydride **3** (see Scheme 1) and to the best of our knowledge has not been previously described. Methacrylic anhydride was chosen as a reagent to obtain a polymerizable methacrylamide handle. The reaction was carried out in water using less than 2 equiv. excess of sodium hydrogen carbonate to drug. The product PENAO MA **4** was separated as a solid and purified by basic aluminium oxide column filtration to remove remaining base and during the reaction produced methacrylic acid. PENAO MA was isolated as a white solid with a yield of 50 %. ¹H and ¹³C NMR spectra (see Figure 1 and Figure S2) confirm the successful synthesis of PENAO MA. The peak **f** in Figure 1A associated with the proton adjacent to the amine group, shifted significantly from 3.73 ppm to 4.34 ppm, suggesting the successful amidation of the methacrylamide handle. Additionally, the appearance of the peaks at 5.73 ppm and 5.45 ppm confirm the existence of vinyl protons, which are characteristic of methacrylamide monomers. Conjugating the amino acid group with a more hydrophobic compound may alter the hydrophilicity of the PENAO monomer, but the monomer remained soluble in water and methanol. In fact, PENAO MA could additionally be dissolved in ethanol, while PENAO shows no solubility in this solvent.

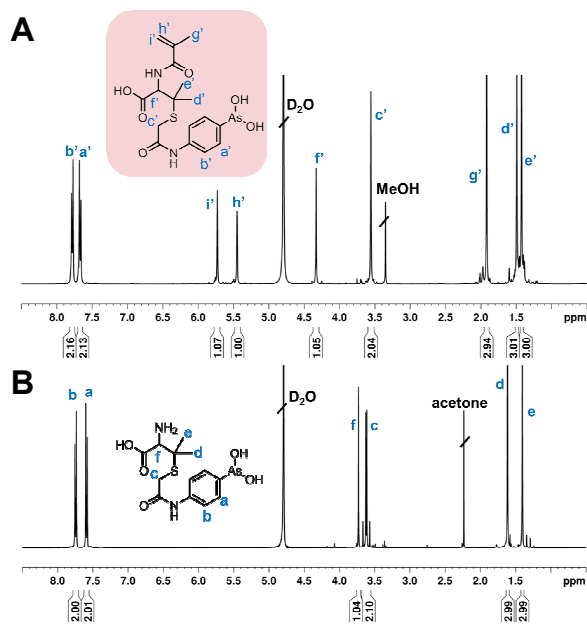


Figure 1. ¹H NMR spectra of PENAO MA 4 (A) and PENAO 2 (B).

PEG-PENAO copolymer synthesis

To exploit PENAO's growth inhibition towards cancer cells when conjugated to a polymer matrix, a copolymer was synthesised. The p(PEG₃₈-co-PENAO₂) polymer was obtained by the RAFT technique³⁴, using CPADB as chain transfer agent, AIBN as initiator and poly(ethylene glycol) methyl ether methacrylate (PEGMA, **7**) and PENAO MA **4** as monomers at a feed concentration ratio [PEGMA: PENAO] : [CPADB] : [AIBN] of 90:10 : 1 : 0.1. The polymerization was carried out in methanol at 70 °C. After 9 hours, the conversion of the copolymerization was determined by ¹H NMR spectroscopy on the crude polymerization mixtures, revealing a copolymer with 38 repeating units of PEGMA and 2 repeating units of PENAO MA. Due to the hydrophilic nature of the copolymer, no particle formation was observed. Instead, p(PEG₃₈-co-PENAO₂) could be dissolved in milli-Q water directly. The copolymer was tested in a SRB assay on 143B sarcoma cells. As previously reported, drug-conjugated polymers have generally a lower cytotoxicity compared to free drugs.³⁵ This is due to the slow diffusion of the polymer across the cell membrane compared to the free drug while the polymers are often too small to display efficient endocytosis. The copolymer p(PEG₃₈-co-PENAO₂) shows negligible cytotoxicity (IC₅₀ = 548.2 μM) towards 143B cells presumably caused by low cellular uptake (see Figure S4). The incorporation of a drug-conjugated polymer into nano-sized structures often enhanced the cytotoxicity of the drug, as it improves cellular uptake by undergoing fast and efficient endocytosis.³⁶ Therefore, an amphiphilic polymer is subsequently prepared that is able to form polymeric micelles with the drug located within the shell to enable direct contact between the drug in the shell and the ANT protein located in the mitochondria membrane, which has shown to be the main target for PENAO.

PMMA-PEG-PENAO copolymer synthesis

PEG based polymers maintain widespread use due to its biocompatibility and clinical establishment.³⁷ The use of p(MMA-*b*-PEG) block copolymers as drug delivery composites are widely known and have shown to be reliable candidates due to their ease to self-assemble into micelle structures as well as being nontoxic at high polymer concentrations.³⁸⁻⁴⁰ This system entails therefore a great platform for the introduction of a new drug PENAO. In addition, it has been reported that micelles with glassy cores are significantly more stable than micelles with soft cores.⁴¹, wherefore methyl methacrylate (MMA, **5**) was chosen as the hydrophobic segment and was subjected to RAFT polymerization mediated by the chain transfer agent CPADB, at different feed concentration ratios [MMA] : [CPADB] : [AIBN] of 100/150/200 : 1 : 0.1. Details on reaction solvent and times, monomer conversions, measured and calculated molecular weight characteristics are compiled in **Table S1**. Three different lengths of poly methyl methacrylate p(MMA) were chosen with the aim of preparing micelles of different sizes. By increasing the hydrophobic content in a block copolymer, more stable micelles can be obtained.⁴² In all cases, polymerizations preceded with similar conversions (determined from ¹H NMR spectroscopy on crude polymerization mixtures) and resulted in monomodal, nearly symmetrical molecular weight distributions with low dispersities $\mathcal{D}_M \leq 1.09$ (see **Figure 2B**, dashed lines).

The p(MMA)-*b*-p(PEG-*co*-PENAO) block copolymers **P1 – 4** (see **Scheme 1**) were obtained *via* RAFT polymerization, using the previous described PMMA macro RAFT agents as chain transfer agents, AIBN as initiator, and PEGMA **7** and PENAO MA **4** as comonomers at a feed concentration ratio [PEGMA: PENAO MA] : [PMMA] : [AIBN] of 80:20/ 180:20 : 1 : 0.1. Two different ratios of PEGMA to PENAO MA (80:20 and 180:20) were compiled to synthesize two block copolymers with different block sizes, but similar amounts of drug (**Table 1**, entry 1 and 2). The polymerizations were carried out at 70 °C, using a solvent mixture of methanol and DMSO due to the different solubility of the hydrophobic macro CTA and hydrophilic PENAO MA. The conversion of the block copolymerizations after 6 hours was determined by ¹H NMR spectroscopy on the crude polymerization mixtures, resulting in block copolymers with 33 to 76 repeating units of PEGMA and ≤ 7 units of PENAO MA. The consumption of PENAO MA is slightly lower than that of PEGMA suggesting a gradient structure of the polymer. It is also interesting to note that the smaller p(MMA) macro RAFT agents with 78 repeating units led to higher conversions of drug monomer, using similar concentration and polymerization time. The influence of the first block on the reactivity ratio of the subsequent copolymerization is known as bootstrap effect.⁴³ The hydrophobic p(MMA) block favours the contact with PEGMA over interaction with the polar PENAO MA. The increased retardation with increasing

PENAO MA feed ratio prevented the incorporation of more than 30-40 wt.% PENAO MA (polymer not shown here) into the polymer without significantly affecting the rate of polymerization at high PENAO MA feed ratios. The block copolymers were purified by dialyses in DMSO and methanol. The exact monomer molar ratios, solvent ratios, monomer conversions and molecular weights characteristics are listed in **Table 1**. ^1H NMR und SEC analysis was used to confirm the successful chain extension of PEGMA and PENAO MA with PMMA. In all cases, polymers with low dispersities $\mathcal{D}_M \leq 1.22$ were obtained for the block copolymers. The SEC traces shifted from lower to higher molecular weights, signifying a clear change in molecular weight (**Figure 2B**). ^1H NMR spectra of purified polymers (example of $\text{p(MMA)}_{78}\text{-}b\text{-p(PEG)}_{33}\text{-}co\text{-PENAO}_7$, **P1**) shown in **Figure 2A** conform to the expected structures. The peaks at 7.65 ppm and 7.83 ppm can clearly be assigned to the phenyl protons of PENAO MA. Moreover, the peak breadth compared to the monomer peak indicates that PENAO MA is bounded to the polymer backbone (**Figure S3**). In addition, the block copolymers were analysed by ICP-MS, showing a similar weight % of arsenic, compared to the calculated wt. % determined from ^1H NMR (**Table 1**). Due to PENAO's high affinity towards thiols it is to mention that no colour change was observed during the reaction, indicating that the pink coloured RAFT thiocarbonylthio end group is still intact.

Table 1 Summary of PENAO MA containing block copolymers prepared by the RAFT process at 70 °C for 6 hours

Entry	Polymer	Monomer feed (mol ratio in %)	Conversion (%)	$M_n^{\text{theo. } a}$ (kg mol $^{-1}$)	$M_n^{\text{SEC } b}$ (kg mol $^{-1}$)	$\mathcal{D}_M^{\text{SEC } b}$	PENAO MA wt.% NMR	ICP-MS
1	$\text{p(MMA)}_{78}\text{-}b\text{-p(PEG)}_{33}\text{-}co\text{-PENAO}_7$ (P1)	PEGMA (80): PENAO (20)	PEGMA (41)/ PENAO (34)	21.2	24.2	1.18	15.34	15.36
2	$\text{p(MMA)}_{78}\text{-}b\text{-p(PEG)}_{76}\text{-}co\text{-PENAO}_6$ (P2)	PEGMA (89): PENAO (11)	PEGMA (42)/ PENAO (27)	33.6	25.6	1.19	8.24	7.62
3	$\text{p(MMA)}_{135}\text{-}b\text{-p(PEG)}_{76}\text{-}co\text{-PENAO}_3$ (P3)	PEGMA (90): PENAO (10)	PEGMA (42)/ PENAO (15)	40.0	39.5	1.22	3.65	4.14
4	$\text{p(MMA)}_{176}\text{-}b\text{-p(PEG)}_{66}\text{-}co\text{-PENAO}_3$ (P4)	PEGMA (90): PENAO (10)	PEGMA (35)/ PENAO (14)	39.1	33.5	1.16	3.54	3.24

^aCalculated from conversion and composition. ^bDetermined by size exclusion chromatography in DMAc.

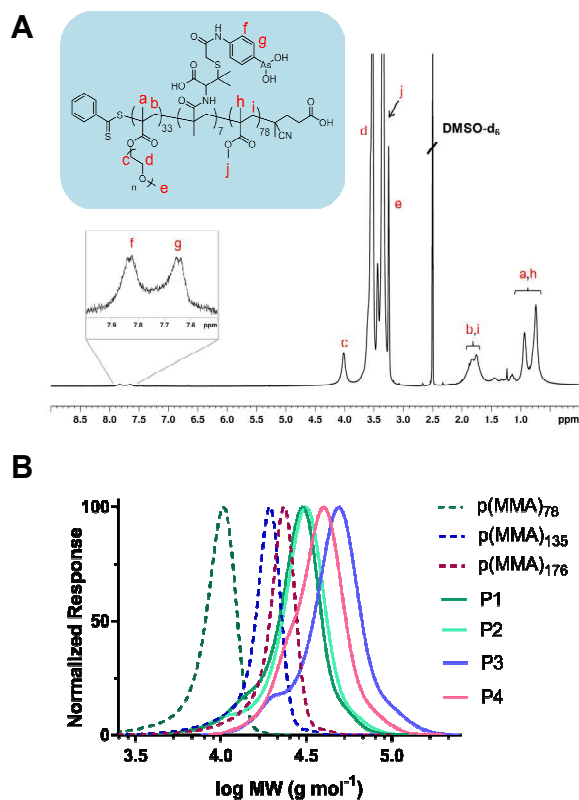


Figure 2. (A) Representative ^1H NMR spectrum of $\text{p(MMA)}_{78}\text{-}b\text{-p(PEG}_{33}\text{-co-PENAO}_7)$ **P1**. (B) SEC traces of p(MMA) macro RAFT agents (dashed curves) and PENAO containing block co polymers $\text{p(MMA)-}b\text{-p(PEG-co-PENAO)}$ (**P1**) $\text{p(MMA)}_{78}\text{-}b\text{-p(PEG}_{33}\text{-co-PENAO}_7)$, (**P2**) $\text{p(MMA)}_{78}\text{-}b\text{-p(PEG}_{76}\text{-co-PENAO}_6)$, (**P3**) $\text{p(MMA)}_{135}\text{-}b\text{-p(PEG}_{76}\text{-co-PENAO}_3)$, (**P4**) $\text{p(MMA)}_{176}\text{-}b\text{-p(PEG}_{66}\text{-co-PENAO}_3)$.

Micelle preparation and their characterization

All block copolymers were only directly soluble in DMSO and DMF, only $\text{p(MMA)}_{78}\text{-}b\text{-p(PEG}_{76}\text{-co-PENAO}_6)$ **P2** could also be dissolved in methanol, due to its 1 : 1 ratio of hydrophobic to hydrophilic block. The micellization of the block copolymers $\text{p(MMA)}_{78}\text{-}b\text{-p(PEG}_{33}\text{-co-PENAO}_7)$ **P1** and **P2** was prepared by adding water to a DMSO or methanol solution respectively, while a DMF solution was used for the block copolymers $\text{p(MMA)}_{135}\text{-}b\text{-p(PEG}_{76}\text{-co-PENAO}_3)$ **P3** and $\text{p(MMA)}_{176}\text{-}b\text{-p(PEG}_{66}\text{-co-PENAO}_3)$ **P4**. Slow addition of water led then to self-assembly into micelles. The micelle solutions were purified by dialysis in water and the remaining solutions were adjusted to 1 mg mL^{-1} working solutions. The size of the micelles was determined by DLS. The block copolymer with the shortest PEG chain (**P1**) led to nanoparticles with the smallest size (**M1**), while **P2 – P4** formed nanoparticles (**M2 – M4**) with similar sizes within errors despite having increasing hydrophobic block length (**Figure 3** and **Table S3**). All micelle systems are monodispersed, showing only one population of particles (**Figure 3A**). This observation was confirmed when visualizing the size and shape of micelles

1
2
3 in dry state *via* transmission electron microscopy (TEM) (**Figure 3B**). Average diameters measured by
4 TEM did not deviate significantly to the measured average diameters determined by DLS, indicating
5 that no aggregate formation is present. Additionally, we observed a rough particle margin. The
6 higher the ratio of arsenic drug to PEGMA, the rougher the margin appears. Zhang *et al.*²⁶ observed a
7 similar phenomenon, when they loading phenylarsine oxide (PAO) into poly(ethylene oxide)-block-
8 poly[α -(6-mecaptohexyl amino) carboxylate- ϵ -caprolactone] PEO-*b*-p(CCLC6-SH) micelles. A control
9 micelle, formed from p(MMA)₁₇₆-*b*-p(PEG)₃₄ **P5** was prepared and analysed *via* TEM, showing
10 spherical particles with a more even particle margin than p(MMA)-*b*-p(PEG-*co*-PENAO) micelles (**see**
11 **Figure S5**). Furthermore, the average particle diameter of p(MMA)₁₇₆-*b*-p(PEG)₃₄ determined from
12 TEM deviates by more than 50 % from the average diameter measured by DLS. Therefore, we
13 hypothesized that the presence of PENAO MA in the hydrophilic shell influences the surface
14 morphology of p(MMA)-*b*-(PEG) particles, which can play an important role during cellular uptake.
15 The surface charge of the four p(MMA)-*b*-p(PEG-*co*-PENAO) and control p(MMA)-*b*-(PEG) micelles
16 were obtained from zeta-potential measurements in water, showing more negative surface charges
17 for PENAO MA containing particles ($\zeta = -33.8 - -27.1$ mV) compared to non PENAO MA containing
18 particles ($\zeta = -17.6$) (**Figure 3**). We also observed the micelle surface to become more negative as a
19 function of an increase in drug amount. Due to the negative surface charge of the p(MMA)-*b*-p(PEG-
20 *co*-PENAO) particles, aggregation is less likely, which is in agreement with DLS and TEM studies.⁴⁴
21
22
23
24
25
26
27
28
29
30
31
32
33
34
35
36
37
38
39
40
41
42
43
44
45
46
47
48
49
50
51
52
53
54
55
56
57
58
59
60

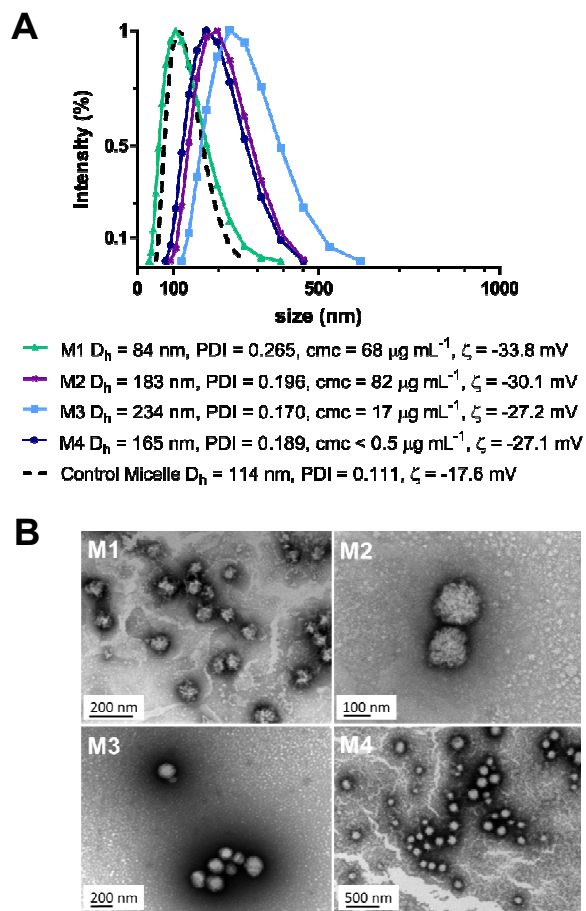


Figure 3. (A) Representative DLS-measured size distributions of PNAO containing nanoparticles (**M1 – M4**) and control micelle and (B) Representative TEM images for PNAO containing nanoparticles (stained with uranyl acetate): **M1** $p(\text{MMA})_{78}\text{-}b\text{-}p(\text{PEG}_{33}\text{-}co\text{-}PNAO_7)$, **M2** $p(\text{MMA})_{78}\text{-}b\text{-}p(\text{PEG}_{76}\text{-}co\text{-}PNAO_6)$, **M3** $p(\text{MMA})_{135}\text{-}b\text{-}p(\text{PEG}_{76}\text{-}co\text{-}PNAO_3)$, **M4** $p(\text{MMA})_{176}\text{-}b\text{-}p(\text{PEG}_{66}\text{-}co\text{-}PNAO_3)$.

The micelle stability was analysed by the determination of the critical micelle concentration (cmc), measuring the scattering intensity for different micelle concentrations ($c = 0 - 100 \mu\text{g mL}^{-1}$) (**Figure S6**).⁴⁵ Micelle stability plays an important role for biological studies. More stable micelle structures directly correlates with a better cellular uptake.³⁸ As expected, an increase of micelle stability was observed with an increase in hydrophobic block length for the less drug containing micelles (**M3** and **M4**), which is in agreement with the literature.⁴⁶ In contrast, **M1** and **M2** with cmc values of $68 \mu\text{g mL}^{-1}$ and $82 \mu\text{g mL}^{-1}$, respectively, are significantly less stable due to the shorter $p(\text{MMA})$ block length, but also the higher drug concentration in the shell. It is known that hydrophobic drugs can improve the thermodynamic stability of micelle systems⁴⁷ but little is known about the effect of hydrophilic drugs on non-crosslinked nanoparticle surfaces. Here we hypothesize that the hydrophilic drug PNAO MA on a polymeric micelle has a detrimental effect on the nanoparticle stability. We assume that the repulsion of the negatively charged PNAO MA chains results in a looser micelle structure, allowing water molecules to migrate closer to the hydrophobic core. A

1
2
3 looser particle structure could also explain the not perfectly round particles, which were revealed by
4 TEM analysis (**Figure 3B**).

6 7 **Activity towards thiols and localization in mitochondria**

8
9 PENAO acts by forming stable cyclic dithioarsenite complexes with two cysteines in the ANT peptide
10 loop.¹⁷ Polymer-drug conjugation is a well-established technique; however the binding of a drug to a
11 carrier can render the drug inactive.⁴⁸ Thus, we exposed **P2** as a model block copolymer, dissolved in
12 DMSO (at a concentration of 1.85 mmol L⁻¹ [PENAO MA groups]) to model monothiols and closely
13 spaced dithiols (monothiol: glutathione (GSH), 3-mercaptopropionic acid (MPA), 2.05-2.1 equiv.
14 relative to [PENAO MA groups]; dithiol: 2,3-dimercaptopropanol (DMP), dithiothreitol (DTT), 1.05
15 equiv. relative to [PENAO MA groups]). Conversions after an incubation time of 24 h were
16 determined by Ellman's assay (thiol concentration plot derived from cysteine hydrochloride
17 standards, **see Figure S7 and S8**) on withdrawn reaction samples. The reaction of **P2** with GSH and
18 MPA reached a conversion of 65 % and 66 %, while the conjugation with DMP and DTT revealed
19 conversions of 90 % and 83 %, respectively. Results are also summarized in **Table 2**. A high selectivity
20 of GSAO – a PENAO mimic with the same reactive arsenous acid residue – towards closely spaced
21 dithiols has been previously reported by Hogg and co-workers.⁴⁹ The trivalent arsenical affinity
22 towards dithiols decreases as a function of an increase in size of the formed As-SH ring structure; the
23 five-membered ring product, formed with DMP reveals a more stable product (dissociation constant
24 DMP = 130 nM) compared to the seven-membered ring product, formed with DTT (dissociation
25 constant DTT = 420 nM) (**Scheme S3**).⁴⁹ A similar trend was observed, when PENAO was subjected to
26 the same thiols, using comparable reaction conditions. By exposing DMP and DTT to PENAO,
27 conversions of 97 % and 80 % were obtained, while the reaction of PENAO and MPA proceeded to a
28 60 % conversion. Almost full conversion (99 %) was reached, when GSH was conjugated to PENAO.
29 The crude PENAO-GSH product was additionally analysed by ¹H NMR spectroscopy, showing no
30 remaining GSH in solution (**Figure S9**). It is yet unclear why PENAOs affinity toward GSH is higher
31 compared to the other examples. It has been previously reported that reduced GSH reacts with
32 As(V) centres by firstly reducing As(V) to As(III) and then binding to the metalloid centre, while for
33 instance 1,2-ethanethiol only selectively conjugates to As(III) compounds.⁵⁰ Dissolved oxygen
34 deactivates the organoarsenous acids by oxidizing the trivalent to the pentavalent state over time.
35 Therefore, we believe a small percentage of PENAO's trivalent As(III) oxidized to its pentavalent
36 As(V), which may result in lower conjugation efficiency for non-reducing thiols. However, we can
37 claim that the thiol-arsenic conjugation proceed on PENAO MA containing polymers as well as on
38 PENAO itself, showing no significant difference in conversion (except PENAO-GSH). With that in
39
40
41
42
43
44
45
46
47
48
49
50
51
52
53
54
55
56
57
58
59
60

mind, we analysed the conjugation behaviour on a model micelle system using **M3** (concentration = 1 mg mL⁻¹) towards the monothiols GSH and MPA. Similar conversions were achieved (**Table 2**, Entry 3 and 7), indicating that the conjugation efficiency between PENAO MA and thiol is the same when on nanoparticle or in free polymer. When increasing the amount of thiols to 10 equiv. to PENAO MA groups, only a minimal increase in conversion (75 -78 %) was observed (**Table 2**, Entry 4 and 8). Additionally, the conjugation product p(MMA)₇₈-*b*-p(PEG₇₆-*co*-PENAO-DMP_{5/6}) (**Table 2**, Entry 10) was purified and analysed by SEC analysis, causing the SEC-measured size distribution to shift minimal to higher molecular weights (**Figure S8**). We interpreted the negligible shoulder in the higher molecular weight region, as the result of thiol-mediated cleavage of RAFT thiocarbonylthio end group producing terminal thiols⁵¹ which can undergo crosslinking by reaction with other polymer chains, or introduce further As-SH conjugation reactions. Nevertheless, no significant change in width or shape was observed, indicating that side reactions were kept to a minimum. It seems therefore that the polymers are still highly reactive towards thiols, which is prerequisite for their activity towards cysteine residues in ANT, which is located on the mitochondria transition pore. To confirm the localization of the PENAO based micelles into the mitochondria, fluorescein *O*-methacrylate was incorporate into the polymer backbone, while the mitochondria of 143B sarcoma cells was stained with the dye Mito Tracker® Deep Red FM and imaged using confocal microscopy (**Figure 4**). The overlapping fluorescence (**Figure 4D**) from Mito Tracker® Deep Red FM (**Figure 4B**) and the fluorescein labelled nanoparticles (**Figure 4A**) confirmed mitochondrial localization of the PENAO carrying micelles. Moreover, this outcome demonstrate that the existence of the negative charges on PENAO nanoparticles ($\zeta = -33.8 - -27.1$ mV) does not hinder the interaction with the mitochondria and PENAO's organoarsinous acid residues still act as an active mitochondrial target when incorporated into a polymeric micelle.

Table 2 Summary of As-SH conjugation products. Conversion was determined by Ellman's assay.

Entry	Compound	Thiol (equiv.)	A ₄₁₂	n (μmol)	Conversion (%)
1	PENAO	GSH (2.05)	0.136	0.294	99
2	P2	GSH (2.05)	0.686	1.480	65
3	M3	GSH (2.05)	0.122	0.261	64
4	M3	GSH (10.0)	0.435	0.931	75
5	PENAO	MPA (2.1)	0.912	2.129	60
6	P2	MPA (2.1)	0.596	1.309	66
7	M3	MPA (2.1)	0.146	0.316	58
8	M3	MPA (10.0)	0.398	0.848	78
9	PENAO	DMP (1.05)	0.079	0.159	97
10	P2	DMP (1.05)	0.330	0.752	90
11	PENAO	DTT (1.05)	0.472	1.089	80
12	P2	DTT (1.05)	0.159	0.324	83

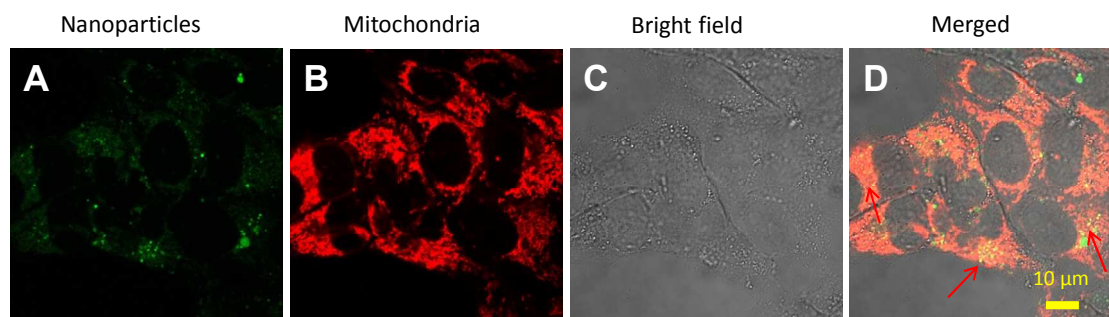


Figure 4. Confocal microscopic images of 143B cells. (A) PNAO nanoparticles (labelled with fluorescein *O*-methacrylate, incubation time 2 hours); (B) Mitochondria (stained with Mito Tracker[®] Deep Red FM, incubation time 30 min); (C) Bright field image of 143B cells; (D) Overlap of green and red fluorescence, indicating mitochondrial localization of the PNAO containing micelles (indicated with red errors). Scale bar 10 μ m.

Cytotoxicity/ cellular uptake studies

With only a few reports on the incorporation of organic arsenicals into synthetic polymers⁵² little is known about their cytotoxicity. Wilson *et al.* recently presented a system of hydrophilic arsenic-functional polymers, with negligible cytotoxicity towards a series of mouse cell lines.⁵⁰ Here, we subjected PNAO, PNAO MA and PNAO MA containing micelles towards human 143B sarcoma cells and explored their cytotoxicity in a SRB assay, which determine the IC_{50} value of the compounds with *in vitro* cultured cells. PNAO's cytotoxicity has been intensively investigated towards an assortment of cell lines showing high growth inhibition with IC_{50} values around the low micro molar range.^{16, 18} The cytotoxicity of free PNAO, PNAO MA and different micelle systems was evaluated *in vitro*. After 72 h of incubation, the IC_{50} of PNAO was determined to be $2.7 \pm 0.3 \mu$ M. Interestingly, the PNAO monomer is significant less cytotoxic ($IC_{50} = 77.9 \pm 7.6 \mu$ M) than PNAO, presumably to the attachment of the methacrylamide handle. Previous studies have shown that the *D*-penicillamine attachment is necessary to improve cellular uptake and to limit the rate of export by the multidrug resistant protein (MRP1/2).¹⁶ All of the here utilized micelle formulations however, had significant lower IC_{50} values than the monomer PNAO MA. The more stable **M3** and **M4** show a similar or enhanced cytotoxicity to PNAO ($IC_{50} = 2.5 \pm 0.04 \mu$ M and $IC_{50} = 0.8 \pm 0.02 \mu$ M, respectively), while the less stable **M1** reveals a higher IC_{50} value of $8.3 \pm 1.6 \mu$ M. **M2** was due to its low stability not further investigated for cytotoxicity and cellular uptake studies. The results of the cytotoxicity assay are depicted in **Figure 5**. Cellular uptake depends strongly on micelle stability and particle size. In general it has been consistently shown that smaller particles have a higher rate of extravasation into permeable tissues and reduced hepatic filtration.⁵³ Cellular uptake studies of micelle systems and PNAO were analysed by ICP-MS measurements after an incubation time of 24 h, revealing the highest uptake (2.71 %) for the most stable micelle **M4**. Thus, the higher cytotoxicity of **M4** can be explained by its higher cellular uptake compared to **M3** (1.57 %). In this matter, micelle

stability seems more important than micelle size; the less stable micelle **M1** (with an average hydrodynamic diameter of 84 nm) has the lowest uptake (0.68 %). In comparison, PENAOs cellular uptake was revealed to be 0.93 %. Cytotoxicity and cellular uptake results are also given in **Table S4**. In summary, the most stable micelle system enhanced cytotoxicity and cellular uptake compared to free PENAO, and this is to best of our knowledge the first covalently bound arsenic containing synthetic polymer system that enhanced the performance of the free drug and displays improved proliferation arrest *in vitro*.

It is of interest to further investigate the oxidation state and develop more stable and less oxygen sensitive nanoparticle formulation that efficiently delivers PENAO to solid sarcoma. **M4** already shows promising anti-proliferation activity towards 143B sarcoma cells and polymeric PENAO nanoparticles are expected to enhance accumulation and retention in target tumour areas and to lower the toxicity towards normal organs compared to the free drug. By attaching PENAO to a polymeric matrix instead of using physical encapsulation, drug leakage can be avoided in the bloodstream. No cleavable linker between polymer backbone and drug was necessary, as the arsonous acid side remains active for conjugation reaction. PENAO has been intensively investigated over the last decade^{16-18, 54-57}; however it has never been used in combination with nanoparticles. The here employed system does not show any degradability in biological environments, it is therefore important to further develop biodegradable PENAO polymeric nanoparticles that evade renal filtration and allow subsequent degradation in the human body.

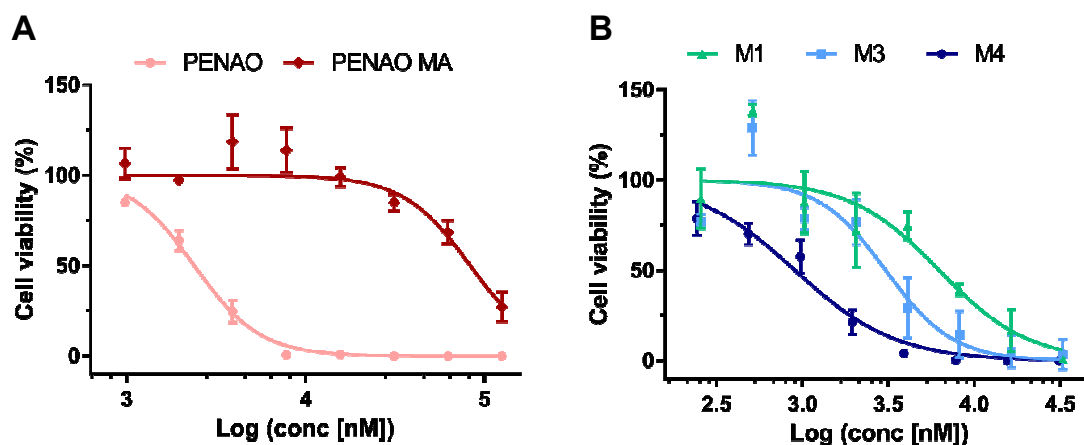


Figure 5. 72 h Cytotoxicity assay on 143B cells of A) PENAO ($IC_{50} = 2.7 \pm 0.3 \mu M$), PENAO MA ($IC_{50} = 77.9 \pm 7.6 \mu M$); B) **M1** ($IC_{50} = 8.3 \pm 1.6 \mu M$), **M3** ($IC_{50} = 2.5 \pm 0.04 \mu M$), **M4** ($IC_{50} = 0.8 \pm 0.02 \mu M$).

Conclusion

In summary, we have demonstrated for the first time that the hydrophilic trivalent organic arsenical drug PENAO is readily available for amidation modifications with methacrylic anhydride to form a polymerizable methacrylamide monomer (PENAO MA), which polymerized *via* the RAFT process with different sized PMMA macro CTAs and in the present of the hydrophilic comonomer PEGMA. In all cases, the PENAO containing polymers self-assembled into micelle structures, leaving PENAO on the particle surface. PENAO's arsenous acid residue remains active when incorporated into a polymer matrix and conjugates to small thiols, showing no significant difference in efficiency between PENAO containing polymers, PENAO containing particles and PENAO itself. Furthermore, the PENAOs moiety allowed localization into the mitochondria of the nanoparticles, and the more stable micelle structures induce growth inhibition in sarcoma cells (143B) and compete with the free drug in terms of cytotoxicity and cellular uptake. This is the first example of PENAO containing nanoparticles, which show great potential for further investigations into the biomedical arena (e.g. in an osteosarcoma animal model) in terms of *in vivo* bio-distribution, anti-cancer efficacy, reduction of side-effects and protein scaffold ability.

Experimental

Materials

All chemicals were purchased as reagent grade from Sigma-Aldrich and used as received unless stated otherwise. Milli-Q water was produced by a Milli-Q water purification system and had a resistivity of 18.2 M Ω .cm. Sodium methoxide was dried over molecular sieve (4 Å). Azobis(isobutyronitrile) (AIBN) was recrystallized from methanol and stored at -24 °C. The monomers methyl methacrylate (MMA) and poly(ethylene glycol) methyl ether methacrylate (PEGMA, monomer molecular weight 300 g mol⁻¹) were passed through basic aluminium oxide (Al₂O₃) to remove inhibitors before polymerization. Deuterated NMR solvents were purchased from Cambridge Isotope Laboratories. The chain transfer agents 4-cyano-4-[(phenylcarbonothioyl)thio]pentanoic acid (CPADB) was prepared as described elsewhere.⁵⁸ Osteosarcoma cell line (143B) was from one of our collaborators Prof. Jia-Lin Yang's laboratory at Sarcoma and Nano-oncology Group (Lowy Cancer Research Centre).

Analysis Techniques

1
2
3 **Nuclear Magnetic Resonance (NMR)** spectroscopic measurements were performed on either a
4 Bruker Avance III 300 MHz (^1H : 300.17 MHz, ^{13}C : 75.48 MHz) or a Bruker Avance III HD 400 MHz (^1H :
5 400.13 MHz, ^{13}C : 100.62 MHz) instrument. Measurements of polymers were done in CDCl_3 , DMSO-d_6
6 or MeOH-d_4 . All other samples were analysed in TFA-d_1 or D_2O . The internal solvent signals $\delta(\text{CDCl}_3)$
7 = 7.26 ppm, $\delta(\text{DMSO-d}_6) = 2.50$ ppm, $\delta(\text{MeOH-d}_4) = 3.31$ ppm, $\delta(\text{TFA-d}_1) = 11.50$ ppm, $\delta(\text{D}_2\text{O}) = 4.79$
8 ppm were used as reference. NMR spectra were processed using either the Bruker TOPSPIN 3.2
9 software or MestReNova NMR software.
10
11

12
13 **Size exclusion chromatography (SEC)** was performed on a Shimadzu system equipped with a $50 \times$
14 7.8 mm guard column and four 300×7.8 mm linear phenogel columns (105, 104, 103 and 500 \AA)
15 operating at a flow rate of 1 mL min^{-1} using *N,N'*-dimethylacetamide (HPLC grade, 0.05% w/v BHT,
16 0.03% w/v LiBr) as eluent. The system was calibrated with a series of narrow molar mass distribution
17 poly(methyl methacrylate) with molar masses ranging from $0.58\text{--}1820 \text{ kg mol}^{-1}$.
18
19

20 **Dynamic light scattering (DLS)** was performed on aqueous solutions (approximately 1 mg mL^{-1}
21 polymer in milli-Q water) which were analysed by a Malvern Zetasizer Nano ZS instrument equipped
22 with a 4 mV He-Ne laser operating at $\lambda = 632 \text{ nm}$ and noninvasive backscatter detection at 173° .
23 Measurements were carried out in a disposable cuvette at 25°C , provided 15 scans equilibration
24 period prior to each set of measurements. For a given sample, a total of three measurements were
25 conducted with the number of runs, attenuator, and path length being automatically adjusted by the
26 instrument, depending on the sample quality.
27
28

29 **Transmission Electron Microscopy (TEM)** was carried out on a JEOL 1400 TEM with a beam voltage
30 of 100 kV and a Gatan CCD for acquisition of digital image. Samples were prepared by depositing 2
31 μL of the aqueous solution mixture onto a copper grid and incubated for 2 min. Excess of the
32 solution mixture was removed and the grids were air dried and negatively stained with $5 \mu\text{L}$ uranyl
33 acetate (UA) solution for 5 min.
34
35

36 **UV-vis** measurements were performed on a Varian Cary 300 Scan spectrophotometer equipped with
37 a Cary temperature controller and a Peltier heating element in quartz cuvettes of 1 cm path length.
38 The measurements were performed at a scan rate of 3000 nm min^{-1} , a wavelength range of 200-800
39 nm, and a standard temperature of 25°C . All samples were diluted with PBS (pH 8) and incubated
40 with $50 \mu\text{L}$ Ellman's reagent solution (0.01 mol L^{-1} in PBS) for 30 min previously to measurement.
41
42

43 **Cell Culture.** 143B (osteosarcoma) cells were grown as monolayer cultures in cell culture flasks by
44 using Dulbecco's Modified Eagle Medium (DMEM) supplemented with 10 % fetal bovine serum
45 (FBS), 1 % glutamax and 100 U mL^{-1} penicillin. The cells in flask were grown in an incubator with a
46 humidified atmosphere at 5 % CO_2 at 37°C . The medium was routinely changed every 3 days. For
47 cell passage and subculture the cell culture media were removed, and cells that have reached
48
49
50
51
52
53
54
55
56
57
58
59
60

1
2
3 confluence were washed with phosphate buffered saline (PBS) and detached by trypsin/EDTA
4 treatment. The cells were then collected, centrifuged, resuspended in the new culture medium and
5 recultured in new flasks.
6

7 **Inductively coupled plasma-mass spectrometry (ICP-MS)** was performed on a Perkin-Elmer NexION
8 300D inductively coupled plasma-mass spectrometer (Perkin-Elmer, Norwalk, CT, USA) to determine
9 quantitative determination of arsenic. All experiments were carried out at an incident radio
10 frequency power of 1500 W. The plasma argon gas flow of 15 L min⁻¹ with an auxiliary argon flow of
11 1.2 L min⁻¹ was used in all cases. The nebulizer gas flow was adjusted to maximize the ion intensity
12 at 1.02 L min⁻¹, as indicated by the mass flow controller. The element/mass detected was ⁹¹AsO (DRC
13 mode) and the internal standard used was ¹⁰³Rh. The replicate time was set to 1000 ms, and the
14 dwell time was set to 100 ms. Peak hopping was the scanning mode employed and the number of
15 sweeps/readings was set to 10. A total of 3 replicates were measured at the normal resolution.
16
17
18
19
20
21
22

23 Experiments

24
25 **Synthesis of 4-(N-(S-penicillaminylacetyl) amino) phenylarsonous acid (PENAO).** PENAO was
26 synthesised in 3 steps according to the procedure of Dilda *et al.*¹⁶ with some modifications: (i) *p*-
27 Arsanilic acid (10.06 g, 46.09 mmol) was suspended in 50 mL milli-Q water and 50 mL of a sodium
28 carbonate solution (7.32 g, 69.09 mmol). The slightly yellow solution was cooled to 0-5°C in an ice
29 bath and bromoacetyl bromide (18.59 g, 8.0 mL, 92.12 mmol) was added over a period of 10 min.
30 The reaction was maintained for 1 h below 20 °C. The precipitated product 4-(2-
31 bromoacetyl-amino)benzenearsonic acid (BRAA) was collected by filtration and washed with water.
32 (ii) The wet cake was then added to a mixture of 75 mL MeOH and 75 mL 48 % hydrobromic acid.
33 Sodium iodide (0.666 g, 4.43 mmol) was added, followed by dropwise addition of a sodium sulfate
34 solution (12.59 g, 88.76 mmol in 65 mL milli-Q water). The heterogeneous mixture was maintained
35 at room temperature for 2.5 hours and then filtered. The residue was suspended in a mixture of
36 methanol (75 mL), 48 % hydrobromic acid (30 mL) and milli-Q water (45 mL), followed by the
37 addition of 75 mL milli-Q water and 75 mL 5 % sodium carbonate solution. The product 4-(2-
38 bromoacetyl-amino)benzenearsonous acid (BRAO) was filtered and dried under reduced pressure
39 (yield: 62 %). ¹H NMR (400 MHz, TFA-d₁): δ/ppm = 7.98 (dd, 4 H, phenyl protons), 4.16 (s, 2 H, BrCH₂-
40). (iii) Under nitrogen atmosphere, 15 mL of anhydrous 25 wt. % sodium methoxide (dried over
41 molecular sieve, 4 Å) and 15 mL anhydrous methanol were weight into a schlenkflask. *D*-
42 penicillamine (0.51 g, 3.43 mmol) was added and the yellow solution was stirred for 5 min at room
43 temperature. Under nitrogen atmosphere BRAO (1.00 g, 3.11 mmol) was then added to the solution
44 and the mixture was stirred for 20 min. The pH was adjusted using 5 % sulfuric acid in methanol to
45
46
47
48
49
50
51
52
53
54
55
56
57
58
59
60

1
2
3 obtain a final pH of 3.6. The heterogeneous solution was filtered and the solvent was removed under
4 reduced pressure. The slightly yellow solid was redissolved in methanol and added dropwise to 50
5 mL of rapidly stirred acetone and left to stir overnight at room temperature. The product was
6 filtered and dried under reduced pressure to obtain PENA0 as colourless solid (yield: 74 %). ¹H NMR
7 (400 MHz, D₂O): δ/ppm = 7.75-7.73 (d, 2 H, -NHphenyl proton, *meta*), 7.60-7.58 (d, 2 H, -NHphenyl
8 proton, *ortho*), 3.73 (s, 1 H, H₂NCHCOOH), 3.62 (q, 2 H, -S(CH₂)CO-), 1.61, 1.40 (s, 6 H, -HCC(CH₃)₂).
9 ¹³C NMR (100.62 MHz, D₂O): δ/ppm = 171.10 (-COOH), 171.00 (-CONHCH-), 144.45 (-NHCphenyl),
10 138.91 (-CAs(OH)₂), 130.10 (-NHphenyl, *meta*), 121.71 (-NHphenyl, *ortho*), 61.38 (-NHCHCOOH),
11 46.82(-CHC(CH₃)₂), 33.17 (-SCH₂-), 26.87, 23.17 (-CHC(CH₃)₂).

12
13
14
15
16
17 **Synthesis of 4-(N-(S-penicillaminylacetyl) amino) phenylarsonous acid methacrylamide (PENA0**
18 **MA)**. PENA0 (450 mg, 1.15 mmol) and sodium hydrogen carbonate (186.9 mg, 2.23 mmol) were
19 dissolved in 7 mL milli-Q water and the solution (pH 7) was cooled to 0-5 °C in an ice bath.
20 Methacrylic anhydride (204.5 mg, 202.5 μL, 1.33 mmol) was added dropwise with vigorous stirring.
21 The mixture was stirred for 2 h while maintaining the temperature of 0-5 °C then stirred overnight at
22 room temperature. The crude solution was added dropwise to 100 mL of rapidly stirred acetone,
23 redissolved in methanol and precipitated again into 50 mL of rapidly stirred acetone. The solvent
24 was removed by decanting and the precipitated colourless solid was redissolved in methanol and
25 filtered through an alumina oxide packed column, before it was dried under reduced pressure (yield
26 50 %). ¹H NMR (400 MHz, D₂O): δ/ppm = 7.80-7.78 (d, 2 H, -NHphenyl proton, *meta*), 7.69-7.67 (d, 2
27 H, -NHphenyl proton, *ortho*), 5.73 (q, 1 H, HHC=C(CH₃-), 5.45 (q, 1 H, HHC=C(CH₃-), 4.34 (s, 1 H, -
28 HNCHCOOH), 3.56 (q, 2 H, -S(CH₂)CO-), 1.92 (s, 3 H, HHC=C(CH₃-), 1.50, 1.43 (s, 6 H, -HCC(CH₃)₂). ¹³C
29 NMR (100.62 MHz, D₂O): δ/ppm = 175.28 (-COOH), 171.80 (-CONHCH-), 170.90 (-H₂C=CONH-), 140.72
30 (-NHCphenyl), 138.83 (-CAs(OH)₂), 130.92 (-NHphenyl, *meta*), 130.45 (H₂C=C(CH₃)), 121.67 (-
31 NHphenyl, *ortho*), 121.47 (H₂C=C(CH₃-), 61.94 (-NHCHCOOH), 48.69 (-CHC(CH₃)₂), 33.31 (-SCH₂-),
32 26.78, 24.61 (-CHC(CH₃)₂), 17.60 (H₂C=C(CH₃)).

33
34
35
36
37
38
39
40
41
42
43 **Copolymerization of PEGMA and PENA0 MA**. PEGMA (147.3 mg, 0.49 mmol, 90 equiv.) and PENA0
44 MA (25.0 mg, 0.055 mmol, 10 equiv.), RAFT agent CPADB (1.52 mg, 0.0055 mmol, 1 equiv.), AIBN
45 (0.90 mg, 0.00055 mmol, 0.1 equiv.) and methanol (0.5 mL, c = 1.08 mol L⁻¹) were mixed in a glass
46 flask, then sealed with a rubber septum, purged with nitrogen for 20 min and placed into a
47 preheated oil bath at 70 °C for 9 h. The polymerization was stopped by quenching to room
48 temperature and monomer conversion and theoretical molecular weights, M_n^{theo.}, were determine
49 by a ¹H NMR spectroscopic measurement of a reaction sample (50-100 μL) diluted with CD₃OH (450
50 μL) by comparison of polymeric signals with the vinyl signals of the residual monomer. The polymer
51 was isolated by dialysis against methanol (regenerated cellulose membranes, MW cut-off 6000-8000
52
53
54
55
56
57
58
59
60

g mol⁻¹) and dried under reduced pressure. The copolymer poly[(polyethylene glycol methyl ether methacrylate)-*co*-4-(*N*-(*S*-penicillaminylacetyl) amino) phenylarsonous acid methacrylamide)], p(PEG₃₈-*co*-PENAO₂) was analysed *via* SEC chromatography. Conversion (PEGMA) = 41 %, conversion (PENAO) = 15 % $M_n^{\text{theo}} = 12.6 \text{ kg mol}^{-1}$, $M_n^{\text{SEC}} = 17.6 \text{ kg mol}^{-1}$, $\bar{M}_w^{\text{SEC}} = 1.13$. The number of repeating units (PEGMA = 38 units; PENAO = 2 units) of p(PEG₃₈-*co*-PENAO₂) was calculated from the monomer conversion obtained from ¹H NMR spectroscopy.

Polymerization of methyl methacrylate (MMA). In a typical experiment, MMA (100, 150, 200 equiv.), RAFT agent CPADB (1 equiv.), AIBN (0.1 equiv.) and solvent (acetonitrile, approx. 1.5 mL mmol⁻¹ of monomer) were mixed in a glass flask, which was sealed with a rubber septum, purged with nitrogen for 25 min and placed into a preheated oil bath at 70 °C for 16-16.5 h. After cooling, polymers were isolated by precipitation into a diethyl ether-hexane mixture (2 : 1), redissolved in chloroform and precipitated again. Details on polymerization times, and polymer characterization by SEC and NMR are summarized in **Table S1**.

Chain extension of PMMA with PEGMA and PENAO MA. PENAO containing block copolymers were prepared by RAFT polymerisation according to the following general procedure. A mixture of PENAO monomer and PEGMA (0.67-1.24 mmol in total), p(MMA) macro RAFT agent (CTA, 1 equiv.), and AIBN (0.1 equiv.) were dissolved in a solvent mixture of DMSO and methanol (approx. total concentration of 0.98-1.13 mol L⁻¹) and combined in a glass flask equipped with a magnetic stir bar. The absolute mass of all reactant and concentrations are given in **Table S2**. The flask was sealed with a rubber septum, purged with nitrogen for 25 min and placed into a preheated oil bath at 70 °C for 6 h. The polymerization was stopped by quenching to room temperature. Monomer conversion and theoretical molecular weights, M_n^{theo} , were determined by a ¹H NMR spectroscopic measurement of a reaction sample (50-100 μL) diluted with DMSO-*d*₆ or MeOH-*d*₄ (450 μL) by comparison of polymeric signals with the vinyl signals of residual monomers. Polymers were purified by dialysis in DMSO and then methanol (regenerated cellulose membranes, MW cut-off 6000-8000 g mol⁻¹). Conversion, SEC data, solvent ratio and mol % feed are given in **Table 1**.

Chain extension of PMMA with PEGMA. PEGMA was chain extended *via* the RAFT process according to the following procedure. PEGMA (0.56 mmol, 200 equiv.), p(MMA) macro RAFT agent (p(MMA)₁₇₆, 1 equiv.), and AIBN (0.2 equiv.) were dissolved in acetonitrile (total concentration of 1.12 mol L⁻¹). The solution was purged with nitrogen for 25 min and then polymerized at 70 °C for 7 h. The polymerization was stopped by quenching to room temperature and monomer conversion and theoretical molecular weights, M_n^{theo} , were determined by a ¹H NMR spectroscopic measurement of a reaction sample (50-100 μL) diluted with CDCl₃ (450 μL) by comparison of polymeric signals with the

1
2
3 vinyl signals of the residual monomer. The polymer was purified two times by precipitation into a
4 diethylether – hexane mixture (4 : 1), dried under reduced pressure and analysed *via* SEC
5 chromatography. The block copolymer poly[(methyl methacrylate)-*b*-(polyethylene glycol methyl
6 ether methacrylate)] (p(MMA₁₇₆)-*b*-p(PEG₄₀), conversion = 20 %, $M_n^{\text{theo}} = 29.9 \text{ kg mol}^{-1}$, $M_n^{\text{SEC}} = 22.7$
7 kg mol^{-1} , $D_M^{\text{SEC}} = 1.15$) was used as a control polymer. The number of repeating units (40 units) of
8 p(PEG) was calculated from the monomer conversion obtained from ¹H NMR spectroscopy.
9
10

11
12 **Formation of Micelles.** The poly[(methyl methacrylate)-*b*-(polyethylene glycol methyl ether
13 methacrylate)-*co*-4-(*N*-(*S*-penicillaminylacetyl) amino) phenylarsonous acid methacrylamide]] or
14 p(MMA)-*b*-p(PEG-*co*-PENAO) block copolymers or p(MMA)-*b*-p(PEG) block copolymers were
15 dissolved in a suitable solvent (DMSO, MeOH or DMF) and milli-Q water was added under rapidly
16 stirring *via* a syringe pump using a rate of 0.2 mL/hour. The solutions were dialysed against milli-Q
17 water for 2 days with frequent water change. The hydrodynamic diameter and zeta potential was
18 measured by dynamic light scattering. The exact polymer feed, solvent ratios, particle sizes,
19 distributions and zeta potentials are listed in **Table S3**.
20
21

22 **Critical Micelle Concentration (CMC).** The CMC was determined by dynamic light scattering
23 measuring the scattering intensity for different micelle concentrations. Briefly, the aqueous micelle
24 solutions (1 mg mL⁻¹) were serially diluted with milli-Q water to obtain concentrations of 0 – 100 µg
25 mL⁻¹. For each sample, a total of two measurements with a 10 scans equilibration period prior to
26 each set of measurements were conducted. The number of runs was set to 11 (run duration 10 sec.),
27 attenuator and path length was fixed to 8 and 4.65.
28
29

30 **Procedure for quantitating sulfhydryl groups using a cysteine hydrochloride standard – Ellman's**
31 **assay.** A thiol calibration plot was prepared using 2.5 mL phosphate buffer (0.1 mmol L⁻¹, pH 8,
32 containing EDTA (1 mmol L⁻¹, 29.2 mg, 0.10 mmol)), 250 µL cysteine hydrochloride standard solution
33 (0 - 1.5 mmol L⁻¹ in PBS) and 50 µL 5'5-dithio-bis-(2-nitrobenzoic acid) (DTNB) solution (10 mmol L⁻¹
34 in PBS). The samples were mixed and incubated for 30 min at room temperature. The UV
35 absorbance of the thiolate ion was then measured at $\lambda = 412 \text{ nm}$ (see **Figure S7**). The thiol
36 concentration was determine from the calibration equation $\lambda_{412} = 1.183[\text{SH}] + 0.01203$.
37
38

39 **Thiol conjugation.** Procedure for PENAO or PENAO block copolymers conjugation reaction: PENAO
40 (1 equiv.) or p(MMA)₇₈-*b*-p(PEG₇₆-*co*-PENAO₆) block copolymer (1 equiv. of PENAO MA groups) was
41 dissolved in PBS (pH 8) (for PENAO) or DMSO (for p(MMA)₇₈-*b*-p(PEG₇₆-*co*-PENAO₆)), (approx. total
42 concentration of 6.0 mmol L⁻¹), and 50 µL thiol stock solution (2.05 - 2.1 equiv. for monothiols
43 (glutathione or 3-mercaptopropionic acid) or 1.05 equiv. for dithiols (2,3-dimercaptopropanol or
44 dithiotreitol), dissolved in PBS or DMSO) was added. The mixture was stirred overnight at room
45
46
47
48
49
50
51
52
53
54
55
56
57
58
59
60

1
2
3 temperature. The conversion of the As-SH conjugation was determine *via* Ellman's assay: 100 μL of
4 sample and 50 μL 5'-dithio-bis-(2-nitrobenzoic acid) (DTNB) solution (10 mmol L^{-1} in PBS) were
5 added to 2.50 mL phosphate buffer (0.1 mmol L^{-1} , pH 8, containing EDTA (1 mmol L^{-1} , 29.2 mg, 0.10
6 mmol)). PNAO-GSH conjugation was additionally analysed *via* ^1H NMR spectroscopy (see Figure S9).
7
8

9
10 Procedure for PNAO nanoparticle conjugation reaction: 1 mL of micelle solution (containing approx.
11 1 mg of polymer $p(\text{MMA})_{135}\text{-}b\text{-}p(\text{PEG}_{76}\text{-}co\text{-}PNAO_3)$ were reacted with glutathione or 3-
12 mercaptopropionic acid (2.05 - 2.1 equiv. to PNAO MA groups) overnight at room temperature. For
13 the Ellman's assay, 250 μL of sample and 50 μL 5'-dithio-bis-(2-nitrobenzoic acid) (DTNB) solution
14 (10 mmol L^{-1} in PBS) were added to 2.5 mL phosphate buffer (0.1 mmol L^{-1} , pH 8, containing EDTA (1
15 mmol L^{-1} , 29.2 mg, 0.10 mmol)).
16
17
18

19
20 All solutions were mixed and incubated for 30 min at room temperature before the UV absorbance
21 of the thiolate ion was measured at $\lambda = 412$ nm. The thiol concentration was determine from the
22 calibration equation $\lambda_{412} = 1.183[\text{SH}] + 0.01203$ (see Figure S8). Results are listed in Table 2.
23
24

25 **IC₅₀ determination via Sulforhodamine B Assay.** Cytotoxicity test and SRB assay of polymeric
26 micelles, PNAO and PNAO MA were determined by a standard sulforhodamine B colorimetric
27 proliferation assay (SRB assay). 143B (osteosarcoma) cells were seeded at a corresponding density
28 of 8,000 cells in 100 μL DMEM media per well in 96-well cell culture plates followed by the addition
29 100 μL of DMEM culture medium per well and incubated at 37 $^{\circ}\text{C}$ in a 5 % CO_2 atmosphere for 24 h.
30 The specimens were sterilized by UV irradiation for 20 min before serially diluting (sequential halved
31 dilution) with sterile water. For the cytotoxicity assay, the medium in the cell culture plate was
32 discarded, and 100 μL of fresh 2 \times concentrated DMEM medium was added to each well of the 96-
33 well culture plate. The sample (PNAO, PNAO MA, M1, M3, or M4) was added into the plate
34 (position 3 A – D to 11 A – D) at 100 μL per well, respectively. Sterile water (100 μL) was added to the
35 non-treated cells into the plate (position 1 A – H, 2 A – H, 3 E – H to 11 E – H, 12 A – G) as a control.
36 The cells were incubated with the micelles or free drug for 72 h, and the cell viability was
37 determined using SRB assay. The incubation with micelles or drug was terminated by the addition of
38 cold trichloroacetic acid (TCA) (10 % w/v) for 30 min at 4 $^{\circ}\text{C}$. After a complete washing with
39 deionised water (5 times), the TCA-fixed cells were stained with 100 μL of 0.4 % w/v sulforhodamine
40 B (SRB) solution in 1 % acetic acid (w/v) for 15 min. After staining, unbound dye was removed by
41 washing with 1 % acetic acid for five times, and plates were air-dried. Finally, the SRB was solubilized
42 with 200 μL of 10 mM Tris buffer to dissolve bounded dye, and the optical density was determined
43 by using a microplate reader at the wavelength of 490 nm. Dose–response curves were plotted
44
45
46
47
48
49
50
51
52
53
54
55
56
57
58
59
60

1
2
3 accordingly where the values were expressed as percentage of control (non-treated cells were used
4 as controls). The optical density was used to calculate cell viability.
5

6 **Cellular Uptake via ICP-MS.** 143B cells were seeded into a 25 cm² flask at 50 x 10⁴ cells per flask and
7 incubated for 48 h. The DMEM medium was replaced by 2 x concentrated DMEM medium and the
8 cells were treated with PENAO polymer micelles (M1, M3, M4) at equal micelle concentrations and
9 free PENAO ($c = 1500 \text{ nmol L}^{-1}$). After 24 h incubation at 37 °C at a 5 % CO₂ atmosphere, the medium
10 was removed and the cells were rinsed with cold PBS (5 mL x 5), trypsinized, collected and rinsed
11 with 9 mL milli-Q water. After drying, the cells were incubated with 50 $\mu\text{L HNO}_3$ (70 %, v/v) at 25 °C
12 for 5 h and then diluted with 10 mL milli-Q water. Arsenic content uptake was determined using
13 inductively coupled plasma mass spectroscopy (ICP-MS). A five-point standard curve was plotted
14 between intensity versus a serial dilution of a certified reference standard ranging from 0.2, 0.5, 1,
15 10, 100 ppb.
16
17
18
19
20
21

22 **Mitochondrial particle localization via confocal microscopy.** To be able to track the mitochondrial
23 localization of the PENAO micelles, 0.2 eq. fluorescein *O*-methacrylate was copolymerized with the
24 comonomers PENAO MA and PEGMA using p(MMA)₁₇₆ as macro RAFT agent and the polymer F-P5
25 (p(MMA)₁₇₆-*b*-p(PEG₇₁-CO-PENAO₂), $M_n^{\text{theo}} = 40.1 \text{ kg mol}^{-1}$, $M_n^{\text{SEC}} = 34.8 \text{ kg mol}^{-1}$, $D_M^{\text{SEC}} = 1.32$) was
26 then self-assembled into micelle structure F-M5, according to the earlier described procedure. The
27 exact polymer feed, solvent ratios, particle sizes, distributions and zeta potentials are listed in **Table**
28 **S3**. For imaging, 143B cells were seeded into a fluoro dish at 10 x 10⁴ cells in 2 mL DMEM medium
29 per dish and incubated at 37 °C at a 5 % CO₂ atmosphere for 24 h. The medium was discarded and
30 the cells were washed with PBS (1 mL x 3) and treated with 100 $\mu\text{g mL}^{-1}$ F-M5 micelle solution in 1
31 mL DMEM medium for 2 h. The medium was discarded and the cells were washed with Hanks'
32 Balanced Salt Solution (HBSS, 1 mL x 3) before 1 mL Mito Tracker[®] Deep Red FM dye (500 nM in
33 HBSS) was added. The cells were incubated for another 30 min with the dye, washed with HBSS (1
34 mL x 2) and imaged using a Zeiss LSM780 confocal microscope. The excitation wavelengths for
35 micelles and Mito Tracker were set as 488 and 633 nm, respectively. The observation was using a
36 100 \times oil objective lens (N.A=1.4) and the images were captured and processed using ZEN software.
37
38
39
40
41
42
43
44
45
46
47

48 Acknowledgements

49
50 The authors acknowledge Ms Sylvia Ganda and Mr Alberto Piloni for Transmission Electron
51 Microscopy assistance. We also like to that the staff of the UNSW Electron Microscopy Unit (EMU)
52 for help. The Mark Wainwright Analytical Centre in acknowledged for performing inductively
53 coupled plasma-mass spectrometry experiments.
54
55

56 There are no conflicts of interest to report
57
58
59
60

ASSOCIATED CONTENT

Details on the MMA polymerization and the chain extension, the formation of micelles, the calculations of the thiol content as well as the As content in the cells can be found in the supporting info. The supporting info includes furthermore NMR analysis of the monomer, cytotoxicity of the statistical copolymer, TEM and stability studies by DLS on the micelle.

Abbreviations

(4-(N-(S-penicillaminylacetyl)amino) phenylarsonous acid) (PENAO); poly(methylmethacrylate) (pMMA); poly(polyethylene glycol methyl ether methacrylate) (PEGMA); methanol (MeOH), dimethylsulfoxide (DMSO); 2,2'-Azobis(2-methylpropionitrile) (AIBN); dynamic light scattering (DLS); nuclear magnetic resonance (NMR); critical micelle concentration (cmc); number-average molecular weight (M_n), dispersity (\mathcal{D}), zetapotential (ζ), polydispersity index from DLS (Pdl); inductively coupled plasma mass spectroscopy (ICP-MS), transmission electron microscopy (TEM),

ORCID

Martina Stenzel: 0000-0002-6433-4419

Philip Hogg: 0000-0001-6486-2863

Notes and References

1. Fricker, S. P., Metal based drugs: from serendipity to design. *Dalton Trans* **2007**, 4903-4917.
2. Lloyd, N. C.; Morgan, H. W.; Nicholson, B. K.; Ronimus, R. S., The Composition of Ehrlich's Salvarsan: Resolution of a Century-Old Debate. *Angew. Chem. Inter. Ed.* **2005**, *44*, 941-944.
3. Koch, R., Report of address at 10th International Medical Congress, Berlin, August 4, 1890. *Dtsch. Med. Wochenschr* **1890**, *16*, 756-757.
4. Dwyer, F. P.; Gyarfas, E. C.; Rogers, W. P.; Koch, J. H., Biological activity of complex ions. *Nature* **1952**, *170*, 190-191.
5. Dwyer, F. P., Inhibition of Landschuetz ascites tumour growth by metal chelates derived from 3,4,7,8-Tetramethyl-1,10-phenanthroline. *Br. J. Cancer* **1965**, *19*, 195-199.
6. Rosenberg B., V. L., Trosko J. E., Mansour V. H., Platinum Compounds: a New Class of Potent Antitumour Agents. *Nature* **1969**, *222*, 385-386.
7. Dilda, P. J.; Hogg, P. J., Arsenical-based cancer drugs. *Cancer Treatment Rev.* **2007**, *33*, 542-564.
8. Ralph, S. J., Arsenic-based antineoplastic drugs and their mechanisms of action. *Met Based Drugs* **2008**, *2008*, 260146.
9. Park, D.; Shon, I. H.; Hua, M.; Chen, V. M.; Hogg, P. J., Visualization of Proteins and Cells Using Dithiol-reactive Metal Complexes. In *Inorganic Chemical Biology*, John Wiley & Sons, Ltd: 2014; pp 215-232.
10. Yan, X.; Li, J.; Liu, Q.; Peng, H.; Popowich, A.; Wang, Z.; Li, X.-F.; Le, X. C., p-Azidophenylarsenoxide: An Arsenical "Bait" for the In Situ Capture and Identification of Cellular Arsenic-Binding Proteins. *Angew. Chem. Int. Ed.* **2016**, *55*, 14051-14056.

11. Huang, C.; Yin, Q.; Zhu, W.; Yang, Y.; Wang, X.; Qian, X.; Xu, Y., Highly selective fluorescent probe for vicinal-dithiol-containing proteins and in situ imaging in living cells. *Angew Chem Int Ed Engl* **2011**, *50*, 7551-7556.
12. Menzel, D. B.; Hamadeh, H. K.; Lee, E.; Meacher, D. M.; Said, V.; Rasmussen, R. E.; Greene, H.; Roth, R. N., Arsenic binding proteins from human lymphoblastoid cells. *Toxicology Lett.* **1999**, *105*, 89-101.
13. Lu, M.; Wang, H.; Wang, Z.; Li, X.-F.; Le, X. C., Identification of Reactive Cysteines in a Protein Using Arsenic Labeling and Collision-Induced Dissociation Tandem Mass Spectrometry. *J. Proteome Res.* **2008**, *7*, 3080-3090.
14. Chen, B.; Liu, Q.; Popowich, A.; Shen, S.; Yan, X.; Zhang, Q.; Li, X.-F.; Weinfeld, M.; Cullen, W. R.; Le, X. C., Therapeutic and analytical applications of arsenic binding to proteins. *Metallomics* **2015**, *7*, 39-55.
15. Peng, Y.; Zhao, Z.; Liu, T.; Li, X.; Hu, X.; Wei, X.; Zhang, X.; Tan, W., Smart Human-Serum-Albumin-As2 O3 Nanodrug with Self-Amplified Folate Receptor-Targeting Ability for Chronic Myeloid Leukemia Treatment. *Angew Chem Int Ed Engl* **2017**, *56*, 10845-10849.
16. Dilda, P. J.; Decollogne, S.; Weerakoon, L.; Norris, M. D.; Haber, M.; Allen, J. D.; Hogg, P. J., Optimization of the Antitumor Efficacy of a Synthetic Mitochondrial Toxin by Increasing the Residence Time in the Cytosol. *J. Med. Chem.* **2009**, *52*, 6209-6216.
17. Park, D.; Chiu, J.; Perrone, G. G.; Dilda, P. J.; Hogg, P. J., The tumour metabolism inhibitors GSAO and PENAO react with cysteines 57 and 257 of mitochondrial adenine nucleotide translocase. *Cancer cell international* **2012**, *12*, 1.
18. Decollogne, S.; Joshi, S.; Chung, S. A.; Luk, P. P.; Yeo, R. X.; Nixdorf, S.; Fedier, A.; Heinzelmann-Schwarz, V.; Hogg, P. J.; Dilda, P. J., Alterations in the mitochondrial responses to PENAO as a mechanism of resistance in ovarian cancer cells. *Gynecologic oncology* **2015**, *138*, 363-371.
19. Chung, S. A.; Decollogne, S.; Luk, P.; Shen, H.; Ha, W.; Day, B.; Stringer, B.; Hogg, P. J.; Dilda, P. J.; Mc Donald, K., PENAO: a Potent mitochondrial targeted inhibitor for glioblastoma. *Neuro-Oncology* **2014**, *16*, v60-v61.
20. Maeda, H., The enhanced permeability and retention (EPR) effect in tumor vasculature: The key role of tumor-selective macromolecular drug targeting. *Advan. Enzyme Regul.* **2001**, *41*, 189-207.
21. Maeda, H.; Bharate, G. Y.; Daruwalla, J., Polymeric drugs for efficient tumor-targeted drug delivery based on EPR-effect. *European Journal of Pharmaceutics and Biopharmaceutics* **2009**, *71*, 409-419.
22. Brannon-Peppas, L.; Blanchette, J. O., Nanoparticle and targeted systems for cancer therapy. *Adv Drug Deliv Rev* **2004**, *56*, 1649-1659.
23. Gothwal, A.; Khan, I.; Gupta, U., Polymeric Micelles: Recent Advancements in the Delivery of Anticancer Drugs. *Pharm Res* **2016**, *33*, 18-39.
24. Qian, C.; Wang, Y.; Chen, Y.; Zeng, L.; Zhang, Q.; Shuai, X.; Huang, K., Suppression of pancreatic tumor growth by targeted arsenic delivery with anti-CD44v6 single chain antibody conjugated nanoparticles. *Biomaterials* **2013**, *34*, 6175-6184.
25. Ahn, R. W.; Chen, F.; Chen, H.; Stern, S. T.; Clogston, J. D.; Patri, A. K.; Raja, M. R.; Swindell, E. P.; Parimi, V.; Cryns, V. L.; O'Halloran, T. V., A novel nanoparticulate formulation of arsenic trioxide with enhanced therapeutic efficacy in a murine model of breast cancer. *Clin Cancer Res* **2010**, *16*, 3607-3617.
26. Zhang, Q.; Vakili, M. R.; Li, X. F.; Lavasanifar, A.; Le, X. C., Polymeric micelles for GSH-triggered delivery of arsenic species to cancer cells. *Biomaterials* **2014**, *35*, 7088-7100.
27. Zhang, Q.; Vakili, M. R.; Li, X. F.; Lavasanifar, A.; Le, X. C., Terpolymer Micelles for the Delivery of Arsenic to Breast Cancer Cells: The Effect of Chain Sequence on Polymeric Micellar Characteristics and Cancer Cell Uptake. *Mol Pharm* **2016**, *13*, 4021-4033.

- 1
- 2
- 3 28. Liu, H.; Zhang, Z.; Chi, X.; Zhao, Z.; Huang, D.; Jin, J.; Gao, J., Arsenite-loaded nanoparticles
- 4 inhibit PARP-1 to overcome multidrug resistance in hepatocellular carcinoma cells. *Sci Rep* **2016**, *6*,
- 5 31009.
- 6 29. Zhang, L.; Xiao, H.; Li, J.; Cheng, D.; Shuai, X., Co-delivery of doxorubicin and arsenite with
- 7 reduction and pH dual-sensitive vesicle for synergistic cancer therapy. *Nanoscale* **2016**, *8*, 12608-
- 8 12617.
- 9 30. Chen, H.; Pazicni, S.; Krett, N. L.; Ahn, R. W.; Penner-Hahn, J. E.; Rosen, S. T.; O'Halloran, T.
- 10 V., Coencapsulation of arsenic- and platinum-based drugs for targeted cancer treatment. *Angew*
- 11 *Chem Int Ed Engl* **2009**, *48*, 9295-9299.
- 12 31. Stenzel, M. H., RAFT polymerization: an avenue to functional polymeric micelles for drug
- 13 delivery. *Chem Commun* **2008**, 3486-3503.
- 14 32. Yoo, H. S.; Lee, E. A.; Park, T. G., Doxorubicin-conjugated biodegradable polymeric micelles
- 15 having acid-cleavable linkages. *Journal of Controlled Release* **2002**, *82*, 17-27.
- 16 33. Larson, N.; Ghandehari, H., Polymeric conjugates for drug delivery. *Chem Mater* **2012**, *24*,
- 17 840-853.
- 18 34. Moad, G.; Rizzardo, E.; Thang, S. H., Living Radical Polymerisation by the RAFT Process. *Aust.*
- 19 *J. Chem.* **2005**, *58*, 379-410.
- 20 35. Blunden, B. M.; Thomas, D. S.; Stenzel, M. H., Macromolecular ruthenium complexes as anti-
- 21 cancer agents. *Polym. Chem.* **2012**, *3*, 2964-2975.
- 22 36. Blunden, B. M.; Lu, H.; Stenzel, M. H., Enhanced delivery of the RAPTA-C macromolecular
- 23 chemotherapeutic by conjugation to degradable polymeric micelles. *Biomacromolecules* **2013**, *14*,
- 24 4177-4188.
- 25 37. Jevsevar, S.; Kunstelj, M.; Porekar, V. G., PEGylation of therapeutic proteins. *Biotechnol J*
- 26 **2010**, *5*, 113-128.
- 27 38. Kim, Y.; Pourgholami, M. H.; Morris, D. L.; Stenzel, M. H., Effect of cross-linking on the
- 28 performance of micelles as drug delivery carriers: a cell uptake study. *Biomacromolecules* **2012**, *13*,
- 29 814-825.
- 30 39. Yu, L.; Yao, L.; You, J.; Guo, Y.; Yang, L., Poly(methyl methacrylate)/poly(ethylene
- 31 glycol)/poly(ethylene glycol dimethacrylate) micelles: Preparation, characterization, and application
- 32 as doxorubicin carriers. *Journal of Applied Polymer Science* **2014**, *131*, 39623-39623.
- 33 40. Cheng, C.; Wei, H.; Zhu, J.-J.; Chang, C.; Cheng, H.; Li, C.; Cheng, S.-X.; Zhang, X.-Z.; Zhuo, R.-
- 34 X., Functionalized Thermoresponsive Micelles Self-Assembled from Biotin-PEG-*b*-P(NIPAAm-*co*-
- 35 HMAAm)-*b*-PMMA for Tumor Cell Target. *Bioconjugate Chem.* **2008**, *2008*, 1194-1201.
- 36 41. Kim, Y.; Liemawal, E. D.; Pourgholami, M. H.; Morris, D. L.; Stenzel, M. H., Comparison of
- 37 Shell-Cross-Linked Micelles with Soft and Glassy Cores as a Drug Delivery Vehicle for Albendazole: Is
- 38 There a Difference in Performance? *Macromolecules* **2012**, *45*, 5451-5462.
- 39 42. Blanazs, A.; Armes, S. P.; Ryan, A. J., Self-Assembled Block Copolymer Aggregates: From
- 40 Micelles to Vesicles and their Biological Applications. *Macromol Rapid Commun* **2009**, *30*, 267-277.
- 41 43. Pai, T. S. C.; Barner-Kowollik, C.; Davis, T. P.; Stenzel, M. H., Synthesis of amphiphilic block
- 42 copolymers based on poly(dimethylsiloxane) via fragmentation chain transfer (RAFT) polymerization.
- 43 *Polymer* **2004**, *45*, 4383-4389.
- 44 44. Mohanraj, V. J.; Chen, Y., Nanoparticles - A review. *Tropical Journal of Pharmaceutical*
- 45 *Research* **2006**, *5*, 561-573.
- 46 45. Callari, M.; Thomas, D. S.; Stenzel, M. H., The dual-role of Pt(IV) complexes as active drug and
- 47 crosslinker for micelles based on β -cyclodextrin grafted polymer. *J. Mater. Chem. B* **2016**, *4*, 2114-
- 48 2123.
- 49 46. Gaucher, G.; Dufresne, M. H.; Sant, V. P.; Kang, N.; Maysinger, D.; Leroux, J. C., Block
- 50 copolymer micelles: preparation, characterization and application in drug delivery. *J Control Release*
- 51 **2005**, *109*, 169-188.
- 52
- 53
- 54
- 55
- 56
- 57
- 58
- 59
- 60

- 1
2
3 47. Chang, T.; Trench, D.; Putnam, J.; Stenzel, M. H.; Lord, M. S., Curcumin-Loading-Dependent
4 Stability of PEGMEMA-Based Micelles Affects Endocytosis and Exocytosis in Colon Carcinoma Cells.
5 *Mol Pharm* **2016**, *13*, 924-932.
- 6 48. Du, A. W.; Lu, H.; Stenzel, M. H., Core-Cross-Linking Accelerates Antitumor Activities of
7 Paclitaxel-Conjugate Micelles to Prostate Multicellular Tumor Spheroids: A Comparison of 2D and 3D
8 Models. *Biomacromolecules* **2015**, *16*, 1470-1479.
- 9 49. Donoghue, N.; Yam, P. T. W.; Jiang, X.-M.; Hogg, P. J., Presence of closely spaced protein
10 thiols on the surface of mammalian cells. *Protein Science* **2000**, *9*, 2436-2445.
- 11 50. Wilson, P.; Anastasaki, A.; Owen, M. R.; Kempe, K.; Haddleton, D. M.; Mann, S. K.; Johnston,
12 A. P. R.; Quinn, J. F.; Whittaker, M. R.; Hogg, P. J., Organic arsenicals as efficient and highly specific
13 linkers for protein/peptide-polymer conjugation. *J. Am. Chem. Soc.* **2015**, *137*, 4215-4222.
- 14 51. Roth, P. J.; Boyer, C.; Lowe, A. B.; Davis, T. P., RAFT polymerization and thiol chemistry: a
15 complementary pairing for implementing modern macromolecular design. *Macromol Rapid Commun*
16 **2011**, *32*, 1123-1143.
- 17 52. García-Serrano, J.; Herrera, A. M.; Pérez-Moreno, F.; Valdez, M. A.; Pal, U., Synthesis of novel
18 ionic polymers containing arsonic acid group. *J. Polym. Sci. Part B: Polym. Phys.* **2006**, *44*, 1627-1634.
- 19 53. Alexis, F.; Pridgen, E.; Molnar, L. K.; Farokhzad, O. C., Factors affecting the clearance and
20 biodistribution of polymeric nanoparticles. *Mol. Pharm.* **2008**, *5*, 505-515.
- 21 54. Shen, H.; Decollogne, S.; Dilda, P. J.; Hau, E.; Chung, S. A.; Luk, P. P.; Hogg, P. J.; McDonald, K.
22 L., Dual-targeting of aberrant glucose metabolism in glioblastoma. *J. Exp. Clin. Cancer Res.* **2015**,
23 *34*:14.
- 24 55. Gang, B. P.; Dilda, P. J.; Hogg, P. J.; Blackburn, A. C., Targeting of two aspects of metabolism
25 in breast cancer treatment. *Cancer Biol Ther* **2014**, *15*, 1533-1541.
- 26 56. Tran, B.; Hamilton, A. L.; Horvath, L.; Lam, M.; Savas, P. S.; Grimison, P. S.; Whittle, J. R.; Kuo,
27 J. C.-Y.; Signal, N.; Edmonds, D.; Hogg, P. J.; Rischin, D.; Desai, J., First-in-man trial of 4-(N-(S-
28 penicillaminylacetyl)amino) phenylarsonous acid (PENAO) as a continuous intravenous infusion
29 (CIVI), in patients (pt) with advanced solid tumours. *Journal of Clinical Oncology* **2016**, *34*, e14025-
30 e14025.
- 31 57. Horsley, L.; Cummings, J.; Middleton, M.; Ward, T.; Backen, A.; Clamp, A.; Dawson, M.;
32 Farmer, H.; Fisher, N.; Halbert, G., A phase 1 trial of intravenous 4-(N-(S-glutathionylacetyl) amino)
33 phenylarsenoxide (GSAO) in patients with advanced solid tumours. *Cancer chemotherapy and
34 pharmacology* **2013**, *72*, 1343-1352.
- 35 58. Roth, P. J.; Collin, M.; Boyer, C., Advancing the boundary of insolubility of non-linear PEG-
36 analogues in alcohols: UCST transitions in ethanol-water mixtures. *Soft Matter* **2013**, *9*, 1825-1834.
37
38
39
40
41
42
43
44
45
46
47
48
49
50
51
52
53
54
55
56
57
58
59
60

Graphical Abstract

